FEBS Letters 589 (2015) 1127–1135

FEBS Letters

journal homepage: www.FEBSLetters.org

miR-889 promotes proliferation of esophageal squamous cell carcinomas through DAB2IP

Yanting Xu [a,1], Jiangtu He [b,1], Yue Wang [a], Xinyi Zhu [a], Qiuhui Pan [b,*], Qiuling Xie [c,*], Fenyong Sun [a,*]

[a] Department of Clinical Laboratory Medicine, Tenth People's Hospital of Tongji University, Shanghai 200072, China
[b] Department of Central Laboratory, Tenth People's Hospital of Tongji University, Shanghai 200072, China
[c] College of Life Science and Technology, Jinan University, Guangzhou 510632, China

ARTICLE INFO

Article history:
Received 18 December 2014
Revised 24 March 2015
Accepted 24 March 2015
Available online 1 April 2015

Edited by Angel Nebreda

Keywords:
miR-889
DAB2IP
Cell proliferation
Esophageal squamous cell carcinoma

ABSTRACT

MicroRNAs have been reported to play critical roles in various cancers, but there has been no study on the role of miR-889 in cancers. Here, we report that over-expression of miR-889 leads to rapid proliferation of EC109 and EC9706 cells in vitro and in vivo by inducing cells into S-phase. Using bioinformatics methods, DAB2IP was further confirmed to be a direct target of miR-889. In addition, the expression of DAB2IP, which was negatively correlated with that of miR-889, was significantly associated with clinicopathological features of ESCC patients. In conclusion, miR-889 is an important regulator in ESCC and both miR-889 and DAB2IP may serve as promising biomarkers and therapeutic targets in patients with ESCC.

1. Introduction

Esophageal squamous cell carcinoma (ESCC) is one of the most malignant gastrointestinal cancers worldwide [1]. Although many antitumor therapies have been used in patients with ESCC, the prognosis and the overall survival remain poor [1,2].

MicroRNAs (miRNAs) are 20-25-nt-long highly conserved non-coding RNAs that bind to sequences within the 3′ untranslated region (3′ UTR) of mRNAs and post-transcriptionally regulate the expression of target genes [3,4]. Recent studies have revealed that microRNAs are involved in a broad range of biological processes through their regulation of complex signal transduction pathways [5,6]. More than 50% of human miRNAs are located at fragile sites and genomic regions involved in cancers and can lead to the dysregulation of oncogenes and tumor suppressors [7]. There have been only two studies on miR-889, one in pulmonary tuberculosis (TB) [8] and one in colorectal cancer, which reported that the underexpression of miR-889 was significantly associated with improved progression-free or overall survival of patients [9], but there have been no studies on the function of miR-889 in ESCC. Thus, we chose to study miR-889.

DOC-2/DAB2 interactive protein (DAB2IP), also known as ASK1 interacting protein (AIP1), located on chromosome 9 (q33.1-q33.3) is a member of the Ras-GTPase activating protein (Ras-GAP) family [10,11]. Most studies of DAB2IP have been conducted in prostate cancer (PCa), and the low expression of DAB2IP has been shown to affect proliferation, survival, apoptosis and EMT through several signaling pathways, including Ras-ERK, ASK-JNK, and PI3K-Akt, in PCa cells [12–14]. Moreover, the downregulation of DAB2IP is correlated with resistance to chemo- and radiotherapy in PCa cells [15,16]. In addition, although the downregulation of DAB2IP is not observed in ESCC, it is seen in bladder cancer [17], hepatocellular carcinoma [18], medulloblastoma [10], lung cancer [19] and pancreatic cancer [20]. DAB2IP downregulation in various cancers results from aberrant epigenetic regulation of its promoter due to DNA hypermethylation and/or histone modification by histone methyltransferase [18,21]. The above data suggest that DAB2IP functions as a tumor suppressor and could be a prognostic factor in cancers.

However, neither the relationship between miR-889 and DAB2IP nor their expression and biological function has been

☆ Author contributions: Fenyong Sun, Qiuhui Pan, Qiuling Xie, Yanting Xu and Jiangtu He contributed to the conception of the study; Yanting Xu and Jiangtu He contributed to data analyses and manuscript preparation; Yanting Xu, Jiangtu He, Yue Wang and Xinyi Zhu performed the experiments and edited the manuscript; Jiangtu He contributed to statistical analysis; Yanting Xu wrote and revised the manuscript; Fenyong Sun, Qiuhui Pan and Qiuling Xie provided financial support. All authors read and approved the manuscript.

* Corresponding authors. Fax: +86 21 66300588 (Q. Pan and F. Sun).
E-mail addresses: labpqh@163.com (Q. Pan), xieqiuling098@163.com (Q. Xie), labsfy@163.com (F. Sun).

[1] The authors contributed equally to the work.

http://dx.doi.org/10.1016/j.febslet.2015.03.027
0014-5793/

explored in ESCC. In this study, we first investigated the function and expression of miR-889 in ESCC cells. We then verified that DAB2IP was a target of miR-889 and correlated with the clinicopathological features of ESCC patients. Altogether, our study suggests that miR-889 is an oncogene of ESCC and could be targeted for cancer therapy.

2. Materials and methods

2.1. Cell culture and clinical specimens

SK-BR-3, PC1, HeLa and HEK293T cell lines were purchased from the Chinese Academy of Science cell bank (Shanghai, China). EC9706, EC109 and KYSE150 cells were kindly provided by the Central Laboratory, Tongji University Affiliated People's 10th Hospital (Shanghai, China). All of the cells were cultured in high-glucose Dulbecco's modified Eagle's medium (DMEM; Hyclone, Logan, UT) supplemented with 10% fetal bovine serum (FBS; Gibco-BRL Life Technologies, Paisley, UK) and antibiotics (100 U/mL penicillin and 100 U/mL streptomycin; Gibco-BRL, USA) at 37 °C with 5% CO_2 in a humidified incubator.

The Institutional Review Board approved the tissue procurement protocol used in study, and the appropriate informed consent was obtained from all patients. Pair-matched tumors and adjacent non-tumor esophageal tissue samples were obtained from the Department of Pathology, Anyang Tumor Hospital, Fourth Affiliated Hospital of Henan University of Science and Technology.

2.2. Plasmid construction

For the luciferase reporter assay, the human wt-3′UTR of the DAB2IP gene was amplified by PCR using the primers in Supplementary Table S1. The cDNA was cloned into the XhoI/NotI site of the psiCHECK2 vector (c8021, Promega, Madison, WI, USA), downstream of the Renilla luciferase gene, to generate the psiCHECK2-wt-DAB2IP-3′UTR vector. The mut-3′UTR of the DAB2IP gene was obtained using a KOD-Plus-Mutagenesis kit (F0936K, TOYOBO, Japan) according to the manufacturer's protocol.

For the DAB2IP-overexpressing plasmid, the human DAB2IP-CDS was amplified using the primers in Supplementary Table S1 and cloned into the XhoI/EcoRI site of the pcDNA3.1 vector.

2.3. Cell transfection

A total of 1.5×10^5 ESCC cells were seeded into 6-well plates 24 h prior to transfection. Lipofectamine 2000 transfection reagent (3 μl) and Opti-MEM Medium (Invitrogen, Carlsbad, CA, USA) were used for the transient transfection of microRNA mimics, Anti-miR inhibitor mimics (Genepharma, Shanghai, China), and si-DAB2IP (AM16708, Life Tech, USA) according to the manufacturer's instructions. The final concentration of microRNA or siRNA used in our study was 50 nM. The transfection of plasmid (pcDNA3.1 and pcDNA3.1-DAB2IP) was similar to that of RNA, except that the cells were seeded at 2.5×10^5/well, and 4 μl Lipofectamine 2000 and 2 μg plasmid were used for the transfection.

2.4. RNA isolation and quantitative reverse transcriptase PCR

Total RNA from patient tissue samples and cell lines was extracted by TRIzol according to the manufacturer's protocol (Invitrogen, USA). Reverse transcription was performed using a PrimeScript RT regent kit (RR037A, Takara Bio Inc., Otsu, Shiga, Japan). The expression of mature miRNAs was assayed using a MicroRNA reverse transcription kit (Promega, Madison, WI, USA). Briefly, 12 μl of a mixture containing 1 μg RNA and DEPC-treated H_2O was held at 65 °C for 3 min and then put on ice immediately. Then, 4 μl of 5× Buffer, 0.5 μl M-MLV, 0.5 μl RNasin, 2 μl dNTPs, 0.5 μl specific stem-loop RT primer and 0.5 μl U6 RT were added into the mixture. The 20 μl reactions were incubated as follows: 20 °C for 10 min, 42 °C for 50 min, 75 °C for 5 min, and held at 4 °C.

cDNA was diluted 1:19 with ddH_2O. cDNA, upstream and downstream primers, SYBR and ddH_2O were added into each well of a 96-well plate according to the protocol of the KAPA SYBR FAST Universal qPCR Kit (KK4601, Kapa Biosystems, MA, USA). The data were measured using an ABI 7900 HT PCR sequencer (Applied Biosystems, Foster city, CA, USA), and gene expression was calculated using the △△Ct method for relative quantization using 18S or U6 as endogenous reference genes. The primers are provided in Supplementary Table S1.

2.5. MTT assay

A total of 1000 cells transfected with synthesized oligonucleotides were seeded into each well of a 96-well plate. After 0 h, 48 h, 72 h, and 96 h, 20 μl MTT was added into each well and incubated at 37 °C for 4 h. The medium was removed, and 150 μl DMSO was added and incubated at 37 °C for 10 min to dissolve the crystals. The absorbance values were read at a wavelength of 490 nm.

2.6. Colony formation assay

A total of 500 cells were seeded into each well of a 6-well plate. Ten days later, the cells were washed with PBS, fixed with 95% ethanol for 10 min and then stained with 0.1% crystal violet for 15 min. Cells were washed with water and then observed by phase contrast microscopy (Leica, German).

2.7. Cell cycle assay

A total of 9×10^4 transfected cells were seeded into 6-well plates and incubated in serum-deprived medium (0.2% FBS) for cell synchronization. Subsequently, cells were harvested at 24 h after incubating with complete medium. The cells were stained with propidium iodide (PI) (550825, BD Biosciences, San Diego, CA, USA) and examined with a FACS flow cytometer. Data were analyzed with ModFit software (BD Biosciences, San Jose, CA, USA).

2.8. EdU assay

A total of 1.2×10^5 transfected cells were plated into 6-well plates, and DNA synthesis was assessed with a Cell-Light™ EdU Apollo®488 In Vitro Imaging Kit (C10310-3, RiboBio, Guangzhou, China). Then, nuclei were stained with DAPI (Invitrogen). Finally, cells were visualized and counted with a fluorescent microscope (Leica, German). The EdU labeling index was calculated as EdU-positive cells/total DAPI-positive cells.

2.9. Western blot

Cells were harvested and lysed in RIPA lysis buffer (Beyotime Institute of Biotechnology, China) containing PMSF, cocktail and PhosStop (Roche Applied Science). Total protein was measured with a BCA Protein Quantitation kit (Beyotime, China). Equivalent amounts of total protein extract were separated by SDS–PAGE gels and transferred to nitrocellulose membranes (Millipore, Billercia, MA, USA). Then, the blots were blocked with 5% fat free milk for 1 h and incubated with primary antibodies for β-actin (Santa Cruz Biotechnology, Inc., USA), DAB2IP (ab87811, Abcam, UK), ERK1/2 (4695), Akt (4691), pERK1/2 (T202/Y204, 4376), and pAkt (Ser473, 4058) (all from Cell Signaling Technologies, Beverly, MA,

USA), followed by incubation with their corresponding goat anti-mouse/rabbit immunoglobulin G secondary antibodies (Licor Co., Lincoln, NE, USA). The membranes were scanned with an Odyssey LI-CDR scanner (BD biosciences, USA), and the gray value was measured using Image J software (National Institutes of Health (NIH), Bethesda, MD, USA).

2.10. Dual luciferase reporter assay

Different forms of DAB2IP 3′-UTR (wt-DAB2IP 3′-UTR; mut-DAB2IP 3′-UTR) were cloned downstream of the Renilla luciferase gene into the psi-CHECK2 vector, and the firefly luciferase gene was used to normalize the reporter activities.

For the luciferase reporter assay, a total of 5×10^5 HEK293T cells were seeded and cultured in 6-well plates the day before transfection. Cells were co-transfected with 2 μg of the constructed plasmid together with 75 nM miR mimics or a scrambled sequence using 4 μl Lipofectamine 2000 according to the manufacturer's protocol (Invitrogen). Cells were lysed and assayed for luciferase activity at 24 h after transfection using a Dual-Luciferase Assay kit (E1910, Promega, Madison, WI, USA).

2.11. Immunohistochemistry

Clinical specimens were fixed in 4% paraformaldehyde for 24 h, dehydrated, embedded in paraffin and sliced into 4 μm sections. The tissue sections were treated with xylene and graded alcohol and then equilibrated in PBS. Endogenous peroxidase was blocked with 3% H_2O_2 diluted in PBS for 10 min. Then, antigen retrieval was performed by boiling slides for 10 min at a high pressure in

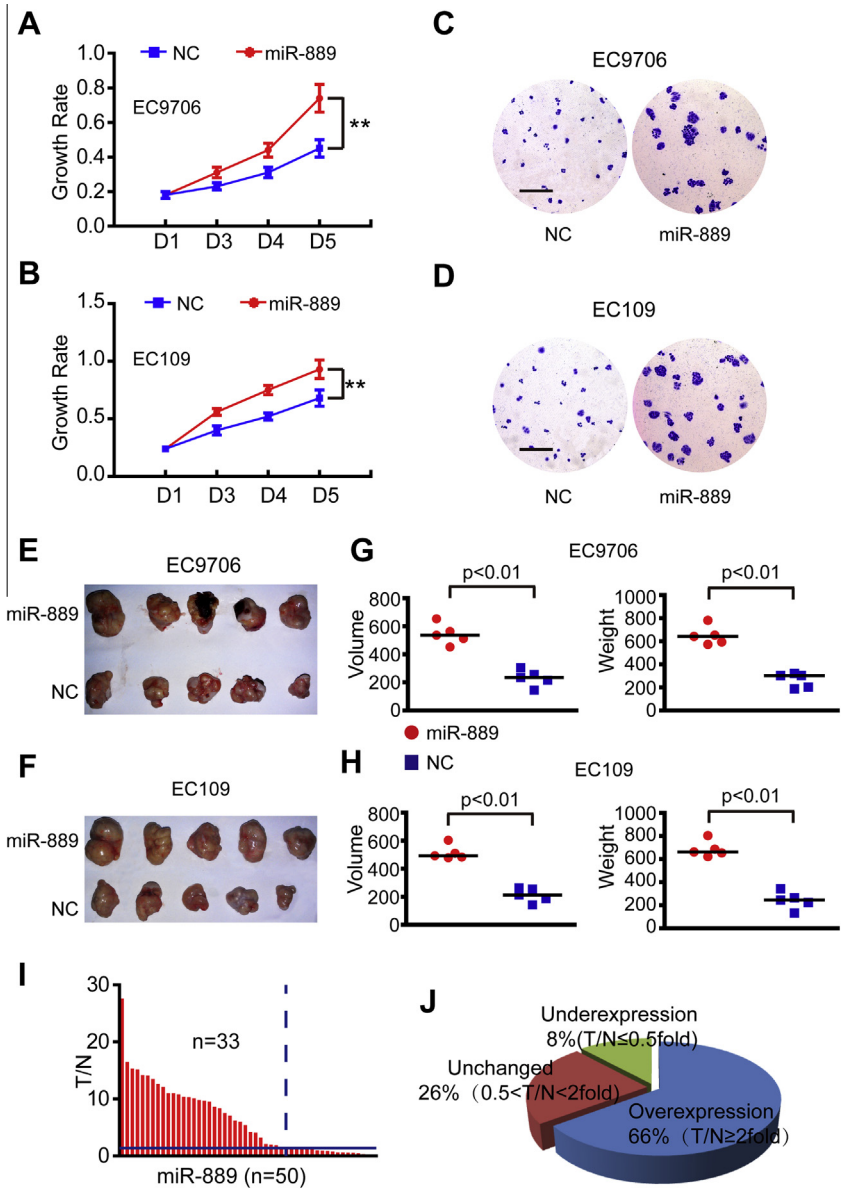

Fig. 1. The functional role and expression of miR-889 in ESCC. (A and B) Growth curves detected at various time points by MTT assay in miR-889-overexpressing and NC subclones generated from EC9706 and EC109 cells. (C and D) The effect of miR-889 overexpression on colony formation. (E–H) The in vivo tumor growth of miR-889 and NC subclones generated from EC9706 and EC109 cells. Five groups were used, and the volume (mm^2) and weight (mg) of tumors were calculated. (I) The ratio of miR-889 expression in human ESCC specimens and corresponding normal tissues (T/N). Fifty pairs of tissues were used for the assay, and the ratio was divided into two parts by T/N = 2 (blue solid line). Thirty-three pairs had a ratio above 2-fold (left of the blue dashed line), and the others had a ratio below 2-fold (right of the blue dashed line) (J) The distribution of miR-889 expression in clinical specimens. The pie was divided into three parts by T/N = 0.5 and T/N = 2.

Improved Citrate Antigen Retrieval Solution (Beyotime, pH 6.0). Non-specific binding was blocked by incubation with normal goat serum (1:500, Invitrogen) for 1 h at room temperature; then, the sections were incubated with anti-DAB2IP antibody (1:200, ab87811, Abcam, UK) at 4 °C overnight. Next, the sections were washed with PBS and incubated with HRP-conjugated secondary antibody (K5007, DAKO, Japan) at room temperature for 1 h. The visualization signal was developed with DAB (DAKO, Japan), and the nuclei were counterstained with hematoxylin (Beyotime). The sections were dehydrated, hyalinized and sealed.

The histologic appearance and staining intensity were examined and scored by two pathologists independently and classified as follows: absent (scored as −), weak-positive (scored as +), moderately-positive (scored as ++) and strong-positive (scored as +++). We classified 2+ or 3+ expression as positive, and + or − expression as negative [22].

2.12. Xenograft tumor model

For the miR-889 overexpression experiments, EC109/EC9706 cells were infected with lentivirus expressing miR-889 (Genchem Limited Company, Changzhou, China) or its negative control at 30–50% confluency. A monoclonal population of stably infected cells was prepared using a limiting dilution assay, and a miR-889-overexpressing clone was selected by qRT-PCR. Then, stable EC109/EC9706-miR-889-LV and EC109/EC9706-NC-LV cells (5×10^6 cells) were inoculated into the left and right flanks of each nude mouse [22–24]. Five mice were included in each group. The weight (mg) was measured with an electronic balance, and the volume of the implanted tumor was measured every 4 days for 4 weeks with a Vernier caliper, using the formula volume (mm^3) = 0.5 × length × $width^2$ [25]. The animal study was performed in strict accordance with the recommendations in the

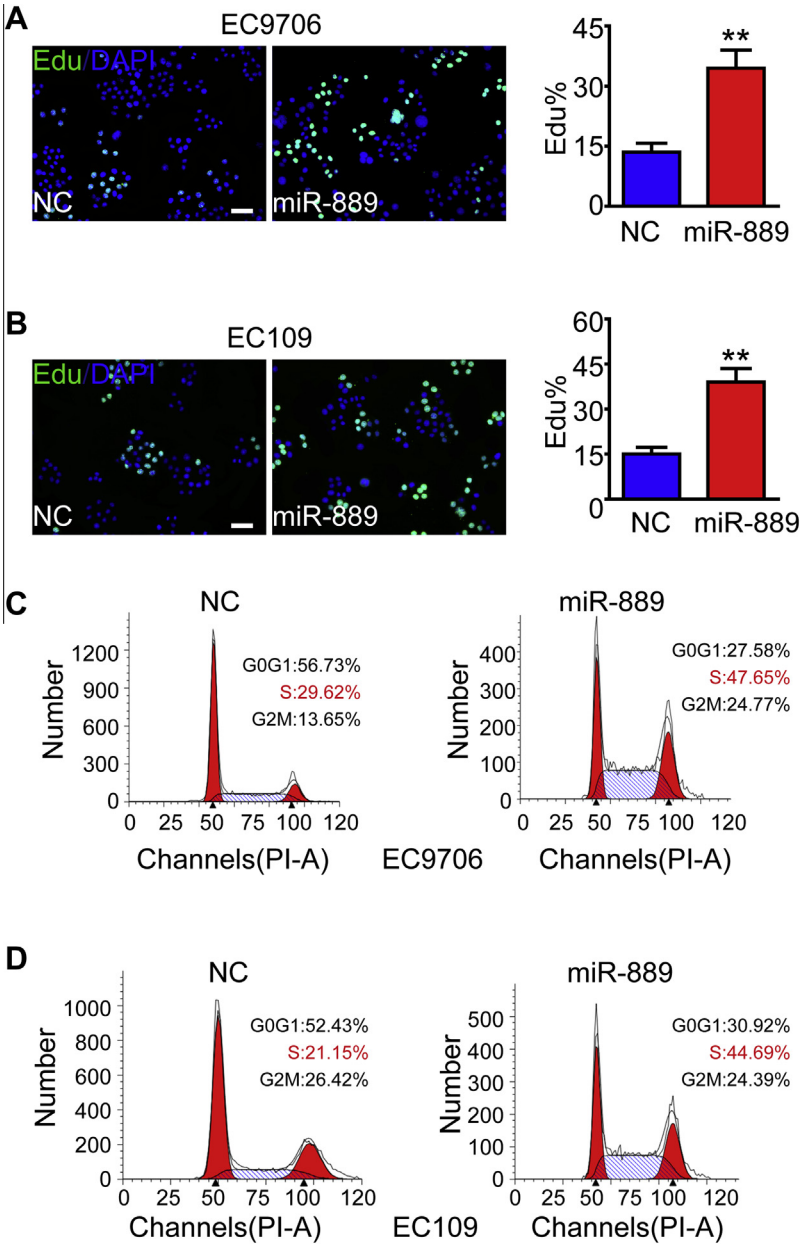

Fig. 2. MiR-889 regulates S-phase cell distribution in ESCC. (A and B) miR-889 enhanced proliferation by promoting the entry of cells into S-phase. The nuclei of cells in S-phase were stained with EdU (green), and the others were stained with DAPI (blue). (C and D) MiR-889 resulted in more S-phase cells. The number of cells in different phases was measured by flow cytometry with PI staining.

guidelines for the Animal Care and Use Committee of the Tenth People's Hospital of Shanghai.

2.13. Statistical analysis

Statistical analyses were performed using SPSS version 21.0 (SPSS Inc., Chicago, IL, USA). All data are presented as the mean ± S.D. Statistical significance is shown as $^{*}(P < 0.05)$, $^{**}(P < 0.01)$, $^{***}(P < 0.001)$.

3. Results

3.1. miR-889 induces proliferation in vitro and in vivo and is overexpressed in clinical specimens

To screen miRNAs that are able to promote or inhibit ESCC cell proliferation, we transfected 300 different miRNAs into EC9706 individually and then detected cell growth by MTT assay. There were 5 miRNAs, miR-221, miR-222, miR-577, miR-1246 and miR-889, that significantly promoted cell proliferation, whereas 6 miRNAs, miR-143, miR-200a, miR-200c, miR-342-5p, miR-510 and miR-940, suppressed cell proliferation. Because very few studies of miR-889 have been reported, we focused on the role of miR-889 in promoting ESCC cell growth. We transfected miR-889 precursor into 3 ESCC cell lines (EC9706, EC109 and KYSE150) to increase the levels of ectopic miR-889 (Supplementary Fig. 1B right, 2A and C, $P < 0.01$) and determined that the elevation of miR-889 significantly increased the growth rate of EC9706 and EC109 from the third day (Fig. 1A and B, $P < 0.01$), whereas in KYSE150, the growth rate increased slowly and there was a difference between NC and miR-889 subclones at the fourth day (Supplementary Fig. 1B left, $P < 0.05$). In addition, the profile of miR-899 expression in the 3 ESCC cell lines was tested, and human embryonic kidney cell 293T was used as control. Compared to 293T, different cell lines were found to express miR-889 to different levels; EC9706 had the lowest expression, followed by EC109, and KYSE150 had the highest (Supplementary Fig. 1A). Based on the qRT-PCR results, a miR-889 inhibitor was used to knockdown endogenous miR-889 in KYSE150 (Supplementary Fig. 1C right, $P < 0.01$), which resulted in a slower growth rate than with the NC (Supplementary Fig. 1C left, $P < 0.05$). Moreover, miR-889 promoted colony formation in EC9706 and EC109 cells (Fig. 1C and D). In conclusion, the overexpression of miR-889 promoted proliferation in ESCC cells. Furthermore, we verified the effect of miR-889 on cell proliferation in 3 additional cancer cell lines (SK-BR-3, PC1 and HeLa), revealing that miR-889 promoted the proliferation of other cancer cells (Supplementary Fig. 3, $P < 0.01$).

To verify the effect of miR-889 in vivo in ESCC cells, miR-889-overexpressing or control cells (Supplementary Fig. 2B and D, $P < 0.01$) were subcutaneously injected into nude mice. Four weeks later, we found that tumors derived from the miR-889 subclone

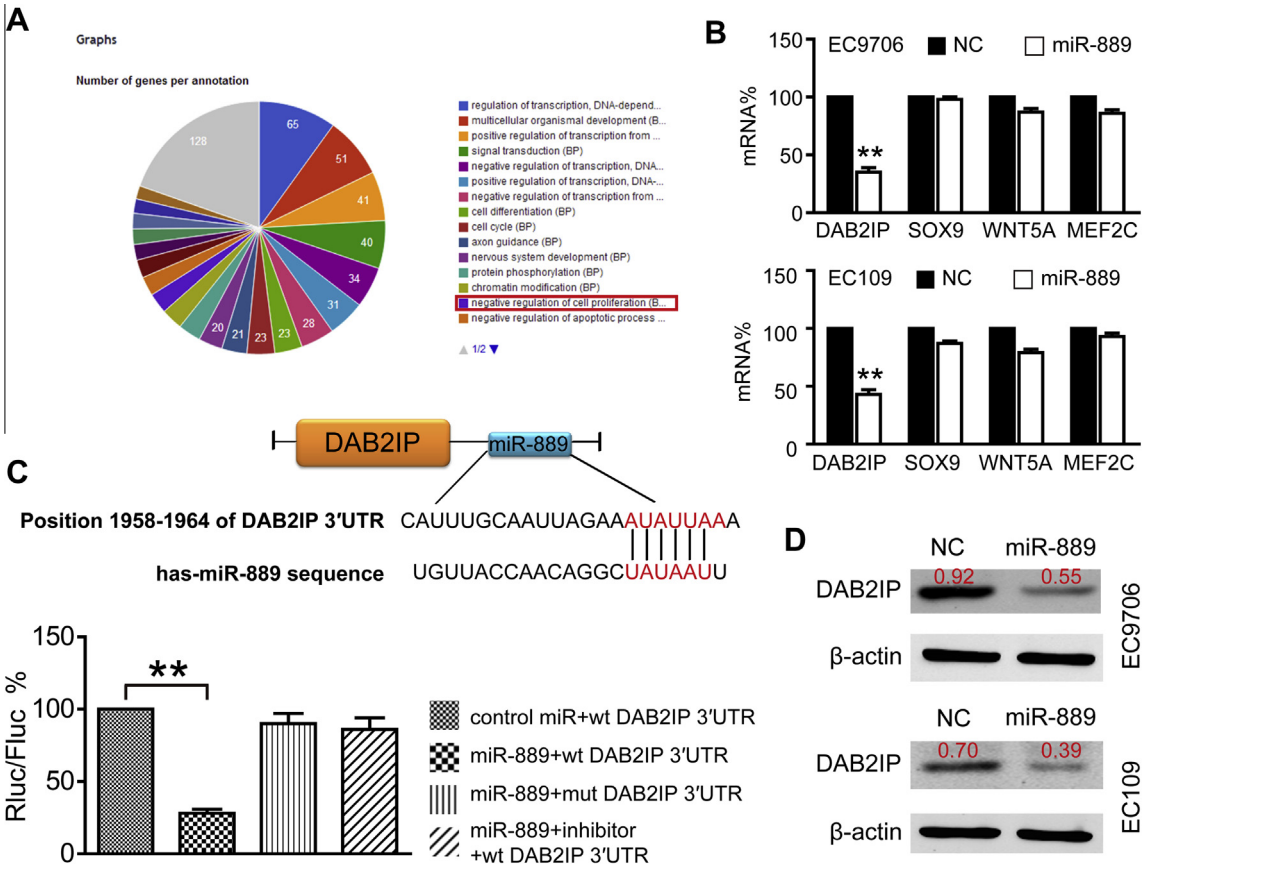

Fig. 3. DAB2IP is the target of miR-889. (A) The distribution of miR-889 target genes. The target genes of miR-889 were divided into groups according to their functions. (B) DAB2IP expression was inhibited by miR-889 at the mRNA level. Four genes (DAB2IP, SOX9, WNT5A and MEF2C) that negatively regulate cell proliferation were chosen to examine the expression level between NC and miR-889 subclones using the 18S ribosome as an internal reference. (C) The binding site of miR-889 within the DAB2IP 3′UTR. The region of the DAB2IP 3′UTR that interacted with miR-889 is identified by TargetScan and highlighted in red. The luciferase activity was measured by dual-luciferase reporter assay and presented as Rluc/Fluc (renilla/luciferase firefly). The Rluc/Fluc value of control was set as 100%. Each experiment was repeated at least three times in triplicate. $^{**}P < 0.01$. (D) miR-889 suppressed the expression of the DAB2IP protein. The expression level of DAB2IP was quantified by western blot using β-actin as an internal reference.

were noticeably larger and heavier than those from the NC subclone (Fig. 1E–H, $P < 0.01$), which demonstrated that miR-889 was also a tumor-promoting factor in vivo. In addition, miR-889 was overexpressed in 66% of the tumor specimens relative to normal tissues (Fig. 1I and J), indicating that the overexpression of miR-889 is associated with ESCC development.

3.2. Overexpression of miR-889 results in a higher percentage of S-phase cells

We showed that miR-889 promoted the proliferation of ESCCs in vitro and vivo and that the proliferation process was always modulated by the cell cycle. Thus, we next determined which step of the cell cycle was influenced by miR-889. First, an EdU assay revealed that the miR-889 subclone incorporated more EdU compared with the NC subclone (Fig. 2A and B, $P < 0.01$), indicating that miR-889 induced cells into S-phase. Moreover, flow cytometry revealed that miR-889 strongly increased the percentage of cells in S-phase (Fig. 2C and D). These data suggested that miR-889 enhanced cell proliferation by affecting the G1-S phase of the cell cycle.

3.3. DAB2IP is a target of miR-889

As it is known that miRNAs work by inhibiting the expression of their target genes, we used TargetScanHuman 6.2 and GeneCoDis3 to predict the targets of miR-889 (Fig. 3A) and then chose four genes (DAB2IP, SOX9, WNT5A and MEGF2C) that had functions that oppose miR-889 in ESCC for our study. Of the 4 genes, only DAB2IP was dramatically inhibited by miR-889 (Fig. 3B, $P < 0.01$). Therefore, DAB2IP was chosen for further research. We determined the miR-889 binding site on the 3′UTR of DAB2IP (Fig. 3C top) and

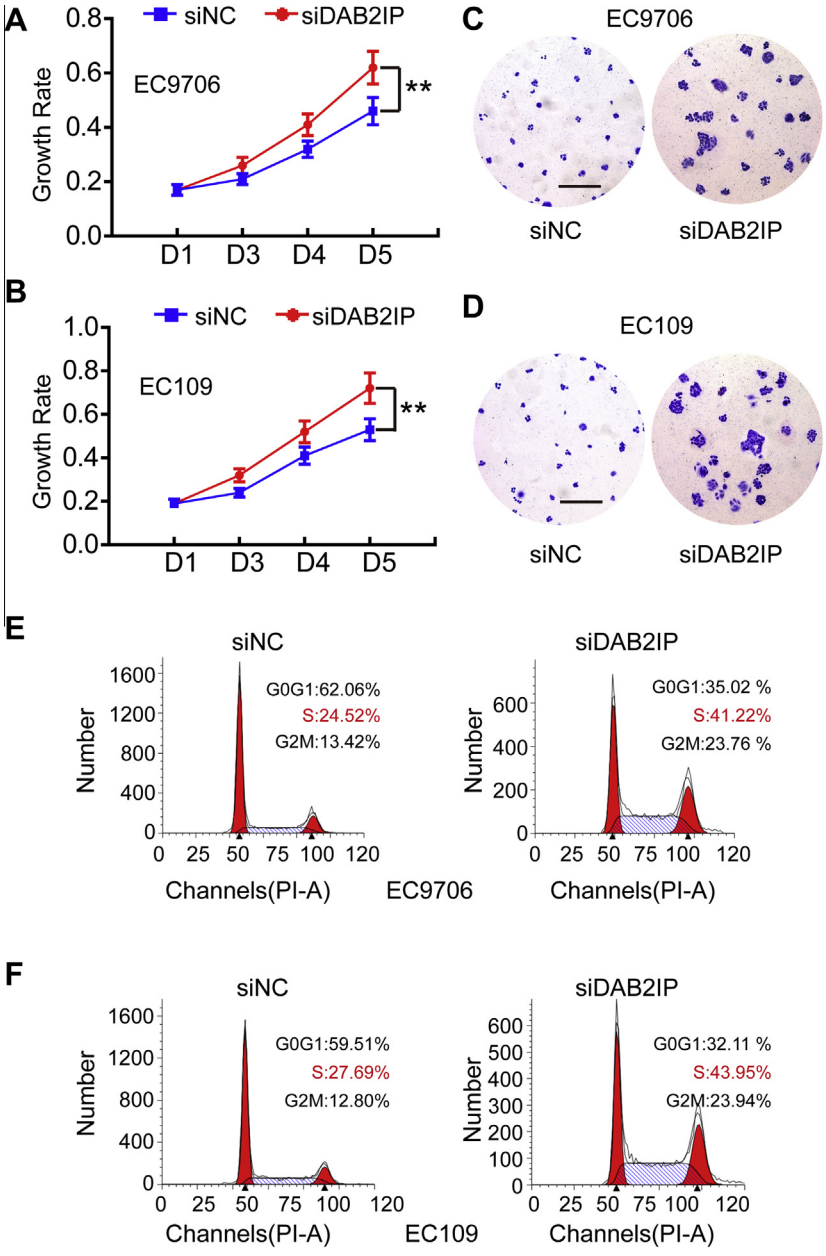

Fig. 4. The knockdown of DAB2IP accelerated the proliferation of ESCC. (A and B) The downregulation of DAB2IP promoted the growth of ESCC. The growth rate was detected by MTT assay. (C and D) DAB2IP affected the formation of ESCC cell colonies. (E and F) The knockdown of DAB2IP resulted in a higher percentage of S-phase cells. Flow cytometry was used to measure the number of cells distributed in different phases.

constructed a 3′UTR mutant DAB2IP plasmid. As shown in Fig. 3C, miR-889 co-transfection dramatically decreased the relative luciferase activity (Rluc/Fluc) of the vector encoding the wt-DAB2IP 3′UTR, but not the vector with mut-DAB2IP 3′UTR. Moreover, the relative luciferase activity (Rluc/Fluc) remained as high as in the control group in the presence of an anti-miR-889 inhibitor. In addition, the expression level of DAB2IP protein in the NC subclone was higher than that in the miR-889 subclone (Fig. 3D), suggesting that miR-889 bound to nucleotides 1958–1964 of the DAB2IP 3′UTR and inhibited its expression.

3.4. Knockdown of DAB2IP accelerates the proliferation of ESCC cells

To determine whether the downregulation of DAB2IP could influence the proliferation of ESCC cells, 3 siDAB2IP sequences (siDAB2IP #1, siDAB2IP #2 and siDAB2IP #3) were used to knock down endogenous DAB2IP, but only one sequence inhibited its expression (Supplementary Fig. 4, $P < 0.01$). Cells transfected with this siDAB2IP appeared to have an increased growth rate (Fig. 4A and B, $P < 0.01$), many large colonies (Fig. 4C and D) and an increased number of cells in S-phase (Fig. 4E and F). Based on the above results, we concluded that decreased DAB2IP could induce the proliferation of ESCC cells, which was in agreement with the effect of miR-889 overexpression. As many studies have reported that DAB2IP regulates the PI3K/Akt and Ras/ERK pathways, which are well characterized and involved in the control of cell proliferation, we verified the expression level of 4 proteins (Akt, p-Akt, ERK1/2 and p-ERK1/2), showing that both of the pathways were activated in siDAB2IP cell lines (Supplementary Fig. 5).

3.5. Rescue of DAB2IP in miR-889 overexpressing cells inhibited proliferation

To test the hypothesis that miR-889 regulates cell proliferation by targeting DAB2IP, EC109 and EC9706 cells were co-transfected with a miR-889 precursor and a DAB2IP-expressing vector. An MTT assay revealed that miR-889 expression increased cell proliferation, whereas this promotion was partially reversed by the co-overexpression of DAB2IP (Fig. 5A and B, $P < 0.01$). Consistently, the increased number of S-phase cells induced by miR-889 was reversed by co-transfection of DAB2IP (Fig. 5C and D, $P < 0.01$). In addition, the qRT-PCR and WB results demonstrated that overexpression of DAB2IP could indeed rescue the expression level of DAB2IP decreased by miR-889 in cells (Supplementary Fig. 6). The observation that the promotion of cell proliferation induced by miR-889 can be reversed by the overexpression of DAB2IP suggested that the effect of miR-889 on cell growth is largely mediated by its effect on DAB2IP.

Table 1
IHC scores of DAB2IP in miR-889 low or miR-889 high group.

	DAB2IPNegative (−/+)	DAB2IPPositive (++/+++)	Total
miR-889 low	4	10	14
miR-889 high	30	6	36
Total	34	16	50

$P < 0.001$.
The relative expression of miR-889 (T/N) was quantified using qRT-PCR and normalized by U6 and DAB2IP was evaluated by IHC staining. The histologic appearance and staining intensity were examined and scored as follows: absent (scored as −), weak-positive (scored as +), moderately-positive (scored as ++) and strong-positive (scored as +++). We classified 2+ or 3+ expression as DAB2IP Positive, and + or − expression as DAB2IP Negative; the samples that T/N < 0.5 as miR-889 low and T/N > 2 as miR-889 high.

3.6. Effect of DAB2IP and miR-889 on the clinicopathological features of ESCC

The expression of DAB2IP was noted mainly in the cytoplasm of cells [17]. In this study, DAB2IP was highly expressed in normal tissues and low-grade ESCC tissues but was expressed at low levels in high-grade ESCC tissues (Fig. 6A). In addition, 83.3% (30/36) of tissues with high expression of miR-889 had low expression of DAB2IP compared with only 28.6% (4/14) of tissues with low

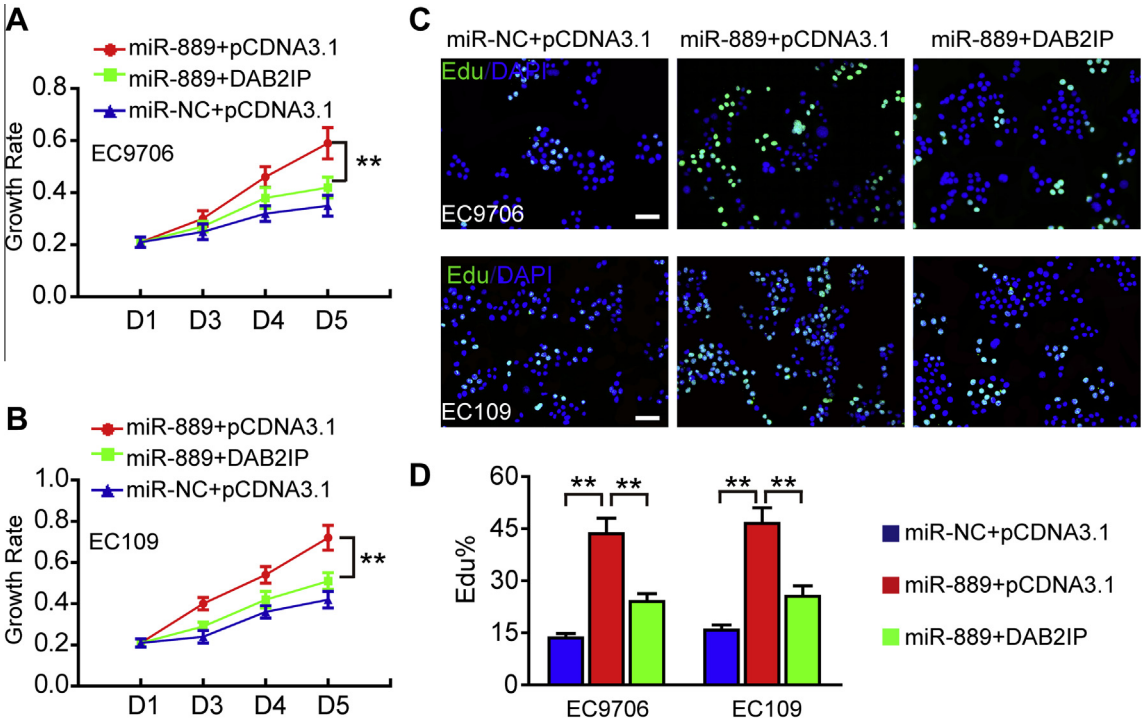

Fig. 5. The rescue of DAB2IP in miR-889-overexpressing cells inhibited proliferation. (A and B) The growth rate was inhibited by the overexpression of DAB2IP in miR-889-overexpressing cells. The data were obtained using the MTT assay at 0 h, 48 h, 72 h and 96 h after transfection. (C and D) The rescue of DAB2IP inhibited proliferation by preventing the entry of cells into S-phase. An EdU kit was used for the assay.

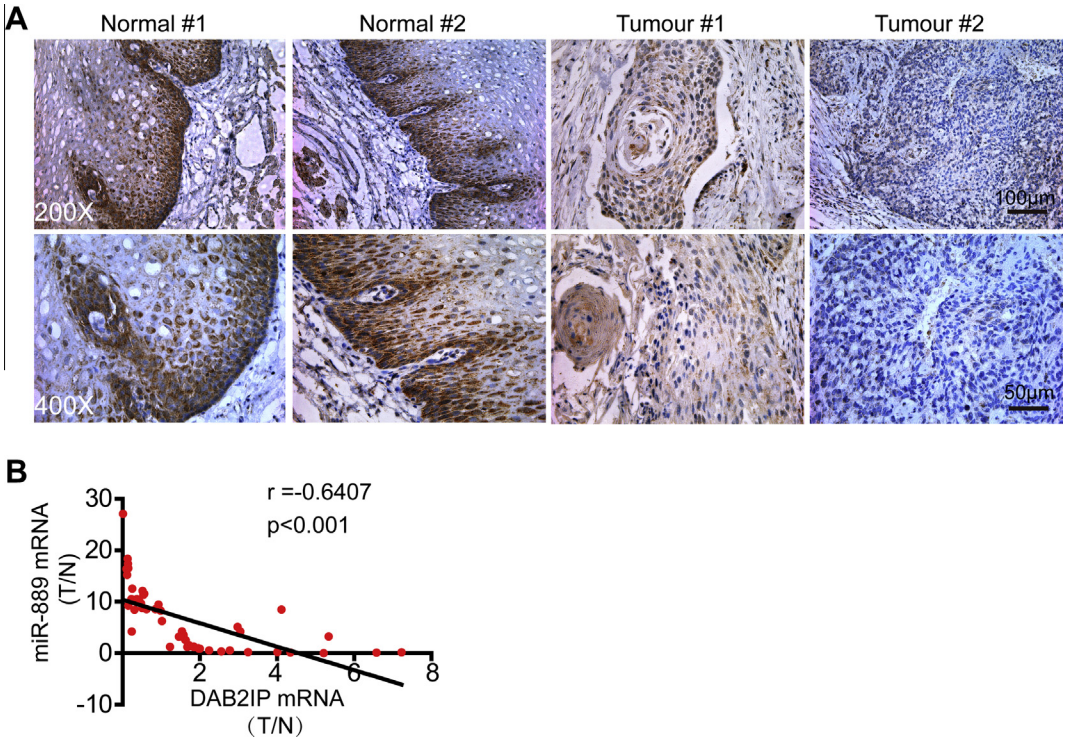

Fig. 6. The correlation between DAB2IP and miR-889 in ESCC tissues and normal esophageal tissues. (A) The expression of DAB2IP in clinical specimens by immunohistochemistry. (B) The negative correlation between the expression of miR-889 and DAB2IP in 50 ESCC patient samples ($r = -0.6407$; $P < 0.001$). The relative expression of miR-889 and DAB2IP was quantified using qRT-PCR, normalized to U6 or 18S and analyzed with the Pearson correlation. For comparisons, a two-tailed, unpaired *t*-test was used.

miR-889 expression (Table 1, $P < 0.001$). Finally, the expression of DAB2IP and miR-889 in the 50 tumor samples analyzed with the Pearson correlation also showed a negative correlation between the two (Fig. 6B, $r = -0.6407$, $P < 0.001$).

The correlation of DAB2IP with the clinicopathologic features of ESCC is shown in Supplementary Table S2. Low expression of DAB2IP was significantly associated with poor differentiation ($P = 0.047$), a high TNM stage ($P = 0.033$) and a large tumor size ($P = 0.003$). No significant associations were found between DAB2IP expression and age, gender, gross pathology, position, or T and N classification ($P > 0.05$).

4. Discussion

The altered expression of miRNAs leading to changes in cell proliferation, survival and apoptosis underlies many diseases, particularly cancers. Various miRNAs have been reported in different cancers. However, to our knowledge, this is the first study to investigate the expression level and biological function of miR-889 in tumors. In this study, we clearly showed that miR-889 functioned as an oncogene that promoted ESCC proliferation, and we verified that DAB2IP was its target gene.

As only one study of miR-889 in tumors, which was in colorectal patients, has been reported, we speculated whether miR-889 had an influence on other types of cancers. Accordingly, the breast cancer cell line SK-BR-3, the prostate cancer cell line PC1 and the cervical cancer cell line HeLa were used for functional research (Supplementary Fig. 3), and their proliferation was also promoted by miR-889, suggesting that miR-889 has a common role in regulating cell proliferation in different types of cancer cells.

DAB2IP is a novel member of the Ras GTPase-activating protein family and is a unique scaffold protein that balances cell proliferation, survival and motility pathways. The N-terminal C2 domain is critical for ASK1 activation pathways, which regulate apoptosis, and the GAP-related domain (GRD) modulates the Ras-mediated signaling pathways [26]. The C-terminal proline-rich (PR) and PERIOD-like (PER) domains are critical for modulating PI3K and Akt activity, respectively [13]. DAB2IP inhibits the Ras pathway by directly binding to and inactivating H-Ras and R-Ras through its Ras GTPase activity, and it regulates the ASK1 pathway by blocking the interaction of ASK1 with its inhibitor 14-3-3 [26,27]. Both the PI3K/Akt pathway (a cascade of anti-apoptotic signals) and the Ras/ERK pathway are well characterized and involved in the control of cell proliferation [28]. Thus, in our study, DAB2IP's role in inhibiting the Ras pathway might explain why the downregulation of DAB2IP by miR-889 can lead to enhancement of ESCC cell proliferation. To confirm this hypothesis, the expression levels of ERK1/2, p-ERK1/2, Akt and p-Akt were assessed by western blotting in cells expressing varying levels of DAB2IP (Supplementary Fig. 5). The knockdown of the endogenous DAB2IP gene by siDAB2IP resulted in increased expression and activation of Akt and ERK1/2, revealing that the two pathways were involved in miR-889-regulated proliferation. In addition, DAB2IP can suppress cancer metastasis by preventing the epithelial-to-mesenchymal transition (EMT) through the inhibition of several pathways, such as the Wnt-β-catenin and Akt-mTOR-ZEB1 pathways [14,29]. Therefore, we speculate that miR-889 may induce EMT through the Akt-ZEB1 pathway.

Although miR-889 was observed to be overexpressed in ESCC cells and tissues, the mechanism remains unknown. There are two main reasons for abnormal versions of microRNAs: one is promoter modification [30] and the other is the regulation of interacting proteins [31,32]; however, which one causes the overexpression of miR-889 should be studied further. There are several pathways leading to the downregulation of DAB2IP in various human cancers: altered epigenetic regulation of its promoter, such as by DNA hypermethylation and/or histone modification [18,21], inactivation through Akt-mediated phosphorylation and

degradation through SCFFbw7-mediated ubiquitination, degradation [12] and inhibition by miR-889, which was verified in our study. Therefore, we speculated that the feedback loop of Akt can enhance the inhibition of DAB2IP by miR-889. However, whether the four DAB2IP downregulation pathways coordinate with each other should be tested in the future.

Overall, miR-889 is an oncogene that regulates the proliferation, survival, migration and invasion of ESCC cells by downregulating DAB2IP, which leads to the alteration of several signaling pathways. Moreover, as DAB2IP is associated with the clinicopathologic features of ESCC and miR-889 is negatively correlated with DAB2IP, they may both serve as potential biomarkers and therapeutic targets in ESCC.

Acknowledgments

This work was supported by China National 973 projects (2012CB966904, 20110402), the Natural Science Foundation of China (81472624, 81272292, 81371913, 81171778) and the Shanghai Health System best academic leader grant.

Appendix A. Supplementary data

Supplementary data associated with this article can be found, in the online version, at http://dx.doi.org/10.1016/j.febslet.2015.03.027.

References

[1] Xing, L. et al. (2014) Definitive chemoradiotherapy with capecitabine and cisplatin for elder patients with locally advanced squamous cell esophageal cancer. J. Cancer Res. Clin. Oncol. 140, 867–872.
[2] Wang, N. et al. (2013) MiR-21 down-regulation suppresses cell growth, invasion and induces cell apoptosis by targeting FASL, TIMP3, and RECK genes in esophageal carcinoma. Dig. Dis. Sci. 58, 1863–1870.
[3] Quintavalle, M. et al. (2010) MicroRNA control of podosome formation in vascular smooth muscle cells in vivo and in vitro. J. Cell Biol. 189, 13–22.
[4] Dang, X. et al. (2012) MicroRNA-26a regulates tumorigenic properties of EZH2 in human lung carcinoma cells. Cancer Genet. 205, 113–123.
[5] Inui, M. et al. (2010) MicroRNA control of signal transduction. Nat. Rev. Mol. Cell Biol. 11, 252–263.
[6] Cordes, K.R. et al. (2009) MiR-145 and miR-143 regulate smooth muscle cell fate and plasticity. Nature 460, 705–710.
[7] Xu, X. et al. (2012) MicroRNA-25 promotes cell migration and invasion in esophageal squamous cell carcinoma. Biochem. Biophys. Res. Commun. 421, 640–645.
[8] Qi, Y. et al. (2012) Altered serum microRNAs as biomarkers for the early diagnosis of pulmonary tuberculosis infection. BMC Infect. Dis. 12, 384.
[9] Molina-Pinelo, S. et al. (2014) MiR-107 and miR-99a-3p predict chemotherapy response in patients with advanced colorectal cancer. BMC Cancer 14, 656.
[10] Smits, M. et al. (2012) EZH2-regulated DAB2IP is a medulloblastoma tumor suppressor and a positive marker for survival. Clin. Cancer Res. 18, 4048–4058.
[11] Wu, K. et al. (2014) The role of DAB2IP in androgen receptor activation during prostate cancer progression. Oncogene 33, 1954–1963.
[12] Dai, X. et al. (2014) Negative regulation of DAB2IP by Akt and SCFFbw7 pathways. Oncotarget 5, 3307–3315.
[13] Xie, D. et al. (2009) DAB2IP coordinates both PI3K-Akt and ASK1 pathways for cell survival and apoptosis. Proc. Natl. Acad. Sci. USA 106, 19878–19883.
[14] Xie, D. et al. (2010) Role of DAB2IP in modulating epithelial-to-mesenchymal transition and prostate cancer metastasis. Proc. Natl. Acad. Sci. USA 107, 2485–2490.
[15] Wu, K. et al. (2013) The mechanism of DAB2IP in chemoresistance of prostate cancer cells. Clin. Cancer Res. 19, 4740–4749.
[16] Kong, Z. et al. (2010) Downregulation of human DAB2IP gene expression in prostate cancer cells results in resistance to ionizing radiation. Cancer Res. 70, 2829–2839.
[17] Shen, Y.J. et al. (2014) Downregulation of DAB2IP results in cell proliferation and invasion and contributes to unfavorable outcomes in bladder cancer. Cancer Sci. 105, 704–712.
[18] Zhang, X. et al. (2012) Low expression of DAB2IP contributes to malignant development and poor prognosis in hepatocellular carcinoma. J. Gastroenterol. Hepatol. 27, 1117–1125.
[19] Yang, L. et al. (2011) A common genetic variant (97906C>A) of DAB2IP/AIP1 is associated with an increased risk and early onset of lung cancer in Chinese males. PLoS One 6, e26944.
[20] Duan, Y.-F. et al. (2013) Decreased expression of DAB2IP in pancreatic cancer with wild-type KRAS. Hepatobiliary Pancreat. Dis. Int. 12, 204–209.
[21] Chen, H. et al. (2005) Down-regulation of human DAB2IP gene expression mediated by polycomb Ezh2 complex and histone deacetylase in prostate cancer. J. Biol. Chem. 280, 22437–22444.
[22] Yuan, X. et al. (2013) Effects and interactions of MiR-577 and TSGA10 in regulating esophageal squamous cell carcinoma. Int. J. Clin. Exp. Pathol. 6, 2651–2667.
[23] Yang, Q. et al. (2014) NRAGE promotes cell proliferation by stabilizing PCNA in a ubiquitin-proteasome pathway in esophageal carcinomas. Carcinogenesis 35, 1643–1651.
[24] Zhang, L. et al. (2011) Effects of cyclooxygenase-2 on human esophageal squamous cell carcinoma. World J. Gastroenterol. 17, 4572–4580.
[25] Ma, J. et al. (2014) Depletion of intermediate filament protein Nestin, a target of microRNA-940, suppresses tumorigenesis by inducing spontaneous DNA damage accumulation in human nasopharyngeal carcinoma. Cell Death Dis. 5, e1377.
[26] Zhang, R. et al. (2003) AIP1 mediates TNF-alpha-induced ASK1 activation by facilitating dissociation of ASK1 from its inhibitor 14-3-3. J. Clin. Invest. 111, 1933–1943.
[27] Wang, Z. et al. (2002) The mechanism of growth-inhibitory effect of DOC-2/DAB2 in prostate cancer. Characterization of a novel GTPase-activating protein associated with N-terminal domain of DOC-2/DAB2. J. Biol. Chem. 277, 12622–12631.
[28] Ewald, J.A. et al. (2013) Expression microarray meta-analysis identifies genes associated with Ras/MAPK and related pathways in progression of muscle-invasive bladder transition cell carcinoma. PLoS One 8, e55414.
[29] Yun, E.J. et al. (2014) DAB2IP regulates cancer stem cell phenotypes through modulating stem cell factor receptor and ZEB1. Oncogene.
[30] He, X.X. et al. (2014) The regulation of microRNA expression by DNA methylation in hepatocellular carcinoma. Mol. Biosyst., http://dx.doi.org/10.1039/c1034mb00563e. in press.
[31] Tanimizu, N. et al. (2014) Downregulation of miR122 by grainyhead-like 2 restricts the hepatocytic differentiation potential of adult liver progenitor cells. Development 141, 4448–4456.
[32] Tian, Y. et al. (2014) MicroRNA-200 cluster regulation by Ascl 2: impact on the epithelial-mesenchymal transition in colon cancer cells. J. Biol. Chem., http://dx.doi.org/10.1074/jbc.M1114.598383. in press.